Veterinary Microbiology 233 (2019) 11–20

Contents lists available at ScienceDirect

Veterinary Microbiology

journal homepage: www.elsevier.com/locate/vetmic

The influence of centrifugation and incubation temperatures on various veterinary and human chlamydial species

Delia Onorini[a,b], Manuela Donati[a], Hanna Marti[b], Roberta Biondi[a], Aurora Levi[a], Lisbeth Nufer[b], Barbara Prähauser[b], Sara Rigamonti[c], Nadia Vicari[c], Nicole Borel[b,*]

[a] DIMES, Microbiology, Policlinico S. Orsola, University of Bologna, Italy
[b] Institute of Veterinary Pathology, Vetsuisse Faculty, University of Zurich, Switzerland
[c] National Reference Laboratory for Animal Chlamydioses, Istituto Zooprofilattico Sperimentale della Lombardia e dell'Emilia Romagna (IZSLER), Pavia, Italy

ARTICLE INFO

Keywords:
Chlamydia
Incubation
Centrifugation
Temperature
Infectivity
Titration by sub-passage

ABSTRACT

The *Chlamydiaceae* are Gram-negative bacteria causing diseases in humans and in both, endothermic (mammals and birds) and poikilothermic (*e.g.* reptiles, amphibians) animals. As most chlamydial species described today were isolated from humans and endothermic animals, the commonly used culturing temperature *in vitro* is 37 °C, although the centrifugation temperature during experimental infection, a technique necessary to improve the infection rate, may vary from 25 to 37 °C. The aim of this study was to investigate the influence of different centrifugation (28° or 33 °C) and incubation temperatures (28 °C or 37 °C) on the average inclusion size, infectivity and ultrastructural morphology of human and animal chlamydial strains, as well as two recently described species originating from snakes, *C. poikilothermis* and *C. serpentis,* in LLC-MK2 cells at 48 h post infection.

Infectivity and average inclusion size was reduced at an incubation temperature of 28 °C compared to 37 °C for all strains including *C. poikilothermis*, although the latter formed larger, fully matured inclusions at 28 °C in comparison to the other investigated *Chlamydia* species. *C.psittaci* displayed a shorter developmental cycle than the other species confirming previous studies. Higher centrifugation temperature increased the subsequent inclusion size of *C. trachomatis*, *C. abortus* and *C. suis* but not their infectivity, while the incubation temperature had no discernable effect on the morphology, inclusion size and infectivity of the other chlamydial strains. In conclusion, we found that all *Chlamydia* species are viable and can grow at low incubation temperatures, although all strains grew better and more rapidly at 37 °C compared to 28 °C.

1. Introduction

The *Chlamydiaceae* are obligate intracellular bacteria that share a unique biphasic developmental cycle. It alternates between two morphological forms, the extracellular, infectious elementary bodies (EBs) and the reticulate bodies (RBs), which divide by binary fission inside of a membrane-bound vacuole termed inclusion before they differentiate back into infectious EBs (AbdelRahman and Belland, 2005). This development is asynchronous and intermediate stages such as intermediate bodies (IBs) and dividing RBs can be observed together with RBs and newly formed EBs (Lee et al., 2018). Adverse environmental conditions can drive these developing chlamydiae into a persistent state, also termed chlamydial stress response, which is characterized by the formation of aberrant bodies (ABs) that remain viable but do not develop into EBs and are therefore non-infectious (Mukhopadhyay et al., 2006).

Members of the *Chlamydiaceae* family are important pathogens causing various diseases in humans and in both, endothermic (mammals and birds) and poikilothermic (*e.g.* reptiles, amphibians) animals. Such a broad host range indicates that *Chlamydiaceae* species may be tolerant for a wide temperature range, which can be mimicked in experimental infection studies *in vitro*.

For example, centrifugation is a commonly used, though sometimes controversially discussed, tool to improve the infection rate *in vitro* based on the induction of cell surface changes (Allan and Pearce, 1979; Lee, 1981; Pearce, 1986; Hodinka et al., 1988). The centrifugation temperature may vary considerably from study to study ranging from 25 °C to 37 °C (Borges et al., 2010; Staub et al., 2018; Wanninger et al., 2016; Marti et al., 2017). It can be hypothesized that the increase of centrifugation temperature may further improve attachment of EBs to host cells. In fact, a previous study on *C. psittaci* demonstrated that centrifugation at 35 °C supported an increased infectivity (46%),

* Corresponding author at: Institute of Veterinary Pathology, Vetsuisse Faculty, University of Zurich, Winterthurerstrasse 268, CH-8057, Zurich, Switzerland.
E-mail address: nicole.borel@uzh.ch (N. Borel).

https://doi.org/10.1016/j.vetmic.2019.04.012
Received 12 February 2019; Received in revised form 9 April 2019; Accepted 10 April 2019
0378-1135/

compared to 20 °C, where the infection rate was lower (27%) (Prain and Pearce, 1989).

In addition, many studies have been conducted using variable incubation temperatures. Usually, the standard temperature for chlamydial infection and incubation is either 35 °C or 37 °C (Kuo and Grayston, 1988; Donati et al., 2010; Joubert and Sturm, 2011), but in a previous study (Staub et al., 2018), incubation temperatures of 28 °C resulted in better growth and isolation of one species (*C. poikilothermis*), but not the other (*C. serpentis*), which grew more successfully at an incubation temperature of 37 °C; both species were isolated from snakes. In contrast, another study showed that an increase of the incubation temperature to 42 °C induced the chlamydial stress response with AB formation in *C. pneumoniae* and further demonstrated that prolonged heat shock treatment for up to 12 or 24 h resulted in the complete loss of infectivity (Mukhopadhyay et al., 2006). Recently, Wannaratana et al. (2017) showed that *C. psittaci*, a zoonotic pathogen originating from birds, could survive at 56 °C for up to 72 h, maintaining its infectivity.

These studies encouraged us to perform a systematic analysis of potential differences in ultrastructural morphology and infectivity of selected chlamydial species upon exposure to various incubation and centrifugation temperatures. In detail, we performed single infections of LLC-MK2 cells with two human chlamydial strains, *C. trachomatis* and *C. pneumoniae*, two known zoonotic chlamydial strains, *C. psittaci* and *C. abortus*, two animal *Chlamydia* species, *C. suis* and *C. pecorum*, as well as two recently described species originating from snakes, *C. poikilothermis* and *C. serpentis*. Inocula were centrifuged and incubated at different temperatures, resulting in three conditions per strain (28 °C centrifugation/ 28 °C incubation (28/28); 28/37; 33/37).

2. Material and methods

2.1. Chlamydial strains

Eight different chlamydial strains were used for this study: two human chlamydial strains, *C. trachomatis* serovar E and *C. pneumoniae* Kajaani 6 (K6), two known zoonotic chlamydial strains, *C. psittaci* 6BCE and *C. abortus* S26/3, two well-described animal strains, *C. suis* 5-27b (SWA-107) from a fattening pig and *C. pecorum* PV7855 from a ruminant (chamois), as well as two recently described snake *Chlamydia* species, *C. poikilothermis* sp. *nov.* and *C. serpentis* sp. *nov.* (Table 1).

2.2. Host cells and media

LLC-MK2 cells (Rhesus monkey kidney cell line, provided by IZSLER, Brescia, Italy) were grown in antibiotic-free growth medium consisting of 500 ml Eagle's minimum essential medium (EMEM, Gibco, Thermo Fisher Scientific, Invitrogen, Carlsbad, CA, United States) supplemented with 10% heat-inactivated fetal calf serum (FCS, BioConcept, Allschwil, Switzerland), 5 ml L-glutamine (Gibco, Thermo Fisher Scientific) and 6 ml glucose (0.06 g/ml; Sigma Aldrich Co., St. Louis, MO, United States). For all infection experiments, growth medium was replaced by *Chlamydia* cultivation medium consisting of 500 ml EMEM supplemented with 20% FCS (BioConcept), 5 ml L-glutamine (Gibco, Thermo Fisher Scientific) and 2 g glucose (Sigma Aldrich) with 0.7 ml cycloheximide (1 mg/ml; Sigma Aldrich) as described (Donati et al., 2010; Wanninger et al., 2016).

2.3. Experimental infection

LLK-MK2 cells, seeded at a density of approximately 1.5×10^5 cells per well and cultivated in 24-well plates overnight, were infected with one of the eight strains at a multiplicity of infection (MOI) of either 1 or 2 aiming for a final infection rate of 20–30% (Fig. S1). Infected monolayers were centrifuged either at 28 °C or 33 °C for 1 h at 2385 *g*. After centrifugation, inocula were replaced with fresh medium at their respective incubation temperature of either 28 °C or 37 °C before incubation with 5% CO_2. Consequently, three conditions were investigated per strain (28 °C centrifugation / 28 °C incubation [28/28]; 28 °C centrifugation / 37 °C incubation [28/37]; 33 °C centrifugation / 37 °C incubation [33/37]).

After an incubation period of 48 h, infected cells were processed either for indirect immunofluorescence microscopy (IFA), titer analysis or transmission electron microscopy (TEM).

2.4. Indirect immunofluorescence microscopy (IFA)

At 48 h post infection (hpi), infected cells were fixed with absolute methanol (-20 °C) for 10 min and chlamydial inclusions were visualized using a *Chlamydiaceae* family-specific mouse monoclonal antibody directed against the chlamydial lipopolysaccharide (LPS, Clone ACI-P, 1:200; Progen, Heidelberg, German) and 1:500 diluted Alexa Fluor 488-conjugated secondary goat anti-mouse antibody (Molecular Probes, Eugene, OR, USA). Host and chlamydial DNA were labelled with 1 µg/ml 4′,6-diamidino-2-phenylindole dihydrochloride (DAPI, Molecular Probes). Coverslips were mounted with FluoreGuard mounting medium (Hard Set; ScyTek Laboratories Inc, Logan, UT, United States) on glass slides and evaluated using a Leica DMLB fluorescence microscope (Leica Microsystems, Wetzlar, Germany) (Staub et al., 2018).

Depending on the inclusion size, a magnification of 100x (oil immersion) or 40x was chosen and the area was measured with either the "Fläche (Kreis) [Area (circle)]" or "Fläche (Polygon) [Area (polygon)]" function, depending on the shape of the inclusion and the area of at least 50 inclusions was measured from each coverslip as described (Staub et al., 2018).

2.5. Titration by sub-passage

Chlamydial titration by sub-passage was evaluated to determine the infectivity of each strain at 37 °C. Following incubation for 48 h, infected monolayers were scraped into 1 ml of supernatant and stored at −80 °C until further processing.

Titration was then performed in LLC-MK2 cells as previously described (Wanninger et al., 2016). Briefly, samples were vortexed for 1 min before serial dilution in incubation medium and then centrifuged for 1 h at 25 °C at 1000 *g*. After centrifugation, inocula were replaced with fresh medium warmed to 37 °C and cultures were incubated at

Table 1
Overview of chlamydial strains used in this study.

Chlamydial Species	Host Species	Strain	Provided by	References
C. trachomatis	Human	Serovar E (Patient P)	DIMES	Donati et al., 2009a,b
C. pneumoniae	Human	K6	IVPZ	Staub et al., 2018
C. psittaci	Human (psittacosis)	6BC	DIMES	Donati et al., 2009a,b
C. abortus	Sheep	S26/3	IZSLER	McClenaghan et al., 1984
C. suis	Pig	5-27b (SWA-107)	IVPZ	Wanninger et al., 2016
C. pecorum	Alpine chamois	PV7855	IZSLER	Magnino et al., 2000
C. serpentis	Snake	H15-1957-10C	IVPZ	Staub et al., 2018
C. poikilothermis	Snake	S15-834 K	IVPZ	Staub et al., 2018

37 °C, 5% CO_2.

48 h post infection (hpi), fixation and immunostaining were performed as described (Staub et al., 2018). The number of inclusions in 30 random microscopic fields was determined for duplicate coverslips per condition using a Leica fluorescence microscope at 200x magnification with a 20x objective (PL FLUOTAR 20x/0.50 PH 2, '/0.17/B). Inclusion forming units (IFU) per ml were then calculated as described (Staub et al., 2018).

2.6. Transmission Electron Microscopy (TEM)

For TEM analysis, cells were fixed with 2.5% glutaraldeyde (Electron Microscopy Sciences, Ft. Washington, USA) for 1 h and embedded in epoxy resin (Fluka, Sigma-Aldrich). For ultrastructural investigation, appropriate areas were selected using semithin sections (1 µm) and stained with toluidine blue (Fluka, Buchs SG, Switzerland). Ultrathin sections (80 nm) were mounted on gold grids (Merck Eurolab AG, Dietlikon, Switzerland), contrasted with uranyl acetate dihydrate (Fluka) and lead citrate (lead nitrate and tri-natrium dihydrate; Merck Eurolab AG) and investigated using a Philips CM10 electron microscope (Staub et al., 2018).

All images were analyzed using the counting tool of the Photoshop CS6 software (Adobe Systems Incorporated, San Jose, CA, USA), to determine the number of elementary bodies (EBs; dark, 0.25–0.5 µm), intermediate bodies (IBs; dark center and pale periphery, equivalent in size to EBs or RBs), reticulate bodies (RBs; pale, 0.5–1 µm), dividing RBs and aberrant bodies (ABs; pale, ≥2 µm) (Marti et al., 2014; Lee et al., 2018) for 10 inclusions per strain and condition.

2.7. Statistical analysis

Results were displayed as means ± standard deviation of the results from three independent experiments. Statistical significance of the difference of means was determined by Student's *t*-test or Welch *t*-test (*t*-test unequal variance), using the Excel software. *p*-values of < 0.05 were considered significant.

3. Results and discussion

Based on morphological characteristics observed in this study, we summarized the investigated species (*C.trachomatis, C. pneumoniae, C. psittaci, C. abortus, C. suis, C. pecorum, C. poikilothermis* sp. *nov.* and *C.serpentis* sp. *nov.*) into two groups and two special cases. The first group comprised *C. pneumoniae*, *C pecorum* and *C. serpentis* (Group 1), while the second group consisted of *C. trachomatis*, *C. abortus* and *C. suis* (Group 2). *C. psittaci* and *C. poikilothermis* were termed special case 1 and special case 2, respectively.

3.1. The average inclusion size was significantly reduced at an incubation temperature of 28 °C compared to 37 °C

We evaluated the average inclusion size and morphology for each strain and condition. Across all strains, we found that the inclusion size post exposure to the 28/28 condition was much smaller (3-25 µm^2) compared to incubation at 37 °C (46-288 µm^2). The only exceptional species was *C. poikilothermis* with notably larger inclusions at 28/28 (25.08 ± 1.97 µm^2) compared to all other species, despite being comparably small compared to inclusions following incubation at 37 °C (62-98 µm^2) (Fig. 1A). We further found that *C. pneumoniae* formed by far the smallest inclusions following an incubation temperature of 37 °C (47.82 ± 3.29 µm^2) while *C. psittaci, C.trachomatis* and *C. suis* had by far the largest inclusions with average inclusion sizes ranging from 236.12 ± 6.17 µm^2 to 282.46 ± 11.07 µm^2 and 288.03 ± 7.42 µm^2, respectively, as observed in previous studies (Escalante-Ochoa et al., 2000; Leonard et al., 2015). The remaining species, *C. serpentis* (121.06 ± 24.45 µm^2), *C. pecorum* (129.90 ± 18.45 µm^2) and *C. abortus* (175.83 ± 28.66 µm^2) all had moderate inclusion sizes at 37 °C as described previously (Staub et al., 2018; Leonard et al., 2015).

Subsequently, we discovered that the average inclusion size for *C. pneumoniae, C.serpentis, C. pecorum*, *C. psittaci* and *C. poikilothermis* was similar between conditions 28/37 and 33/37, whereas the inclusion size significantly increased from 28/37 to 33/37 for *C. trachomatis, C. suis* and *C. abortus* (Fig. 1B, Fig. S2). This notable difference between strains was the basis for the above-mentioned grouping of *C. pneumoniae, C.serpentis* and *C. pecorum* into Group 1 and *C. trachomatis, C. suis* and *C. abortus* into Group 2. *C. psittaci* was considered as a special case because of the considerable inclusion size difference to Group 1 at 37 °C (˜240 µm^2 compared to 46-129 µm^2) and because its developmental cycle has been demonstrated to be much shorter (Hatch et al., 1986; Escalante-Ochoa et al., 2000) than for all other strains investigated in this study. *C. poikilothermis* was another special case due to its notable inclusion size at 28/28 and its peculiar morphology as recently shown (Staub et al., 2018).

In detail (Fig. 1B), Group 1, here represented by *C. pneumoniae*, had smaller inclusion sizes at 28/28 compared to 28/37 or 33/37, with an average of 3.71 ± 0.6 µm^2 at 28/28, 46.32 ± 3.37 µm^2 at 28/37 and 47.83 ± 3.30 µm^2 at 33/37.

Group 2, exemplified by *C. trachomatis*, was significantly reduced at 28/28 compared to 28/37 and 33/37, with an average inclusion size of 4.02 ± 0.47 µm^2, 247.06 ± 13.1 µm^2 and 282.47 ± 11.08 µm^2 for 28/28, 28/37 and 33/37, respectively. The difference between 28/37 and 33/37 was small but significant ($p < 0.05$).

For *C. psittaci* (special case 1), we found a markedly decreased inclusion size at 28/28 compared to the other conditions, with an average size of 3.64 ± 1.09 µm^2 at 28/28, 242.45 ± 3.48 µm2 at 28/37 and 236.12 ± 6.17 µm^2 at 33/37.

C. poikilothermis (special case 2) had small inclusions at 28/28 (25.08 ± 1.97 µm^2) with an increase of inclusion size from 28/37 (62.01 ± 6.10 µm^2) to 33/37 (98.8 ± 47.85 µm^2), which was not significant.

Furthermore, the inclusion morphology was qualitatively assessed for each strain (Fig. 1B, Fig. S2). While the inclusions of all investigated strains, with the exception of *C. poikilothermis*, were regular and round after incubation at 37 °C, the inclusions at 28/28 tended to be small and dot-shaped. In contrast, *C. poikilothermis* presented large and fully formed inclusions at 28 °C which grew even bigger at 37 °C. Moreover, this strain presented an unusual morphology in all conditions, with inclusions of heterogeneous appearance, mostly elongated and growing around the host cell nucleus in a crescent-like fashion. In a previous study investigating two new chlamydial species isolated from snakes (*C. serpentis*, *C. poikilothermis*) and using the human *C. pneumoniae* strain K6 as comparison, the same strains were grown and propagated at both temperatures (28 °C and 37 °C). In that study, we observed a similar pattern for *C. serpentis* and *C. pneumoniae* (tiny inclusions at 28 °C, better growth at 37 °C) as in this study but contrasting results for *C. poikilothermis* (Staub et al., 2018). Specifically, the average inclusions size of *C. poikilothermis* was significantly smaller at an incubation temperature of 37 °C compared to 28 °C and formed inclusions that contained aberrant bodies (ABs) (Staub et al., 2018). In this present study, we found no AB formation in *C. poikilothermis* at 37 °C by immunofluorescence or TEM analysis.

C. psittaci displayed round or oval, lobed inclusions at 37 °C According to Spears and Storz (1979), upon inclusion enlargement, one or more compact lobes develop that later grow together near the host cell nucleus. The lobed structure is a result of division of inclusions occurring in parallel with the multiplication of RBs early in the developmental cycle. The division of inclusions slows or stops in mid-cycle and dividing RBs accumulate within the enlarging lobes (Rockey et al., 1996).

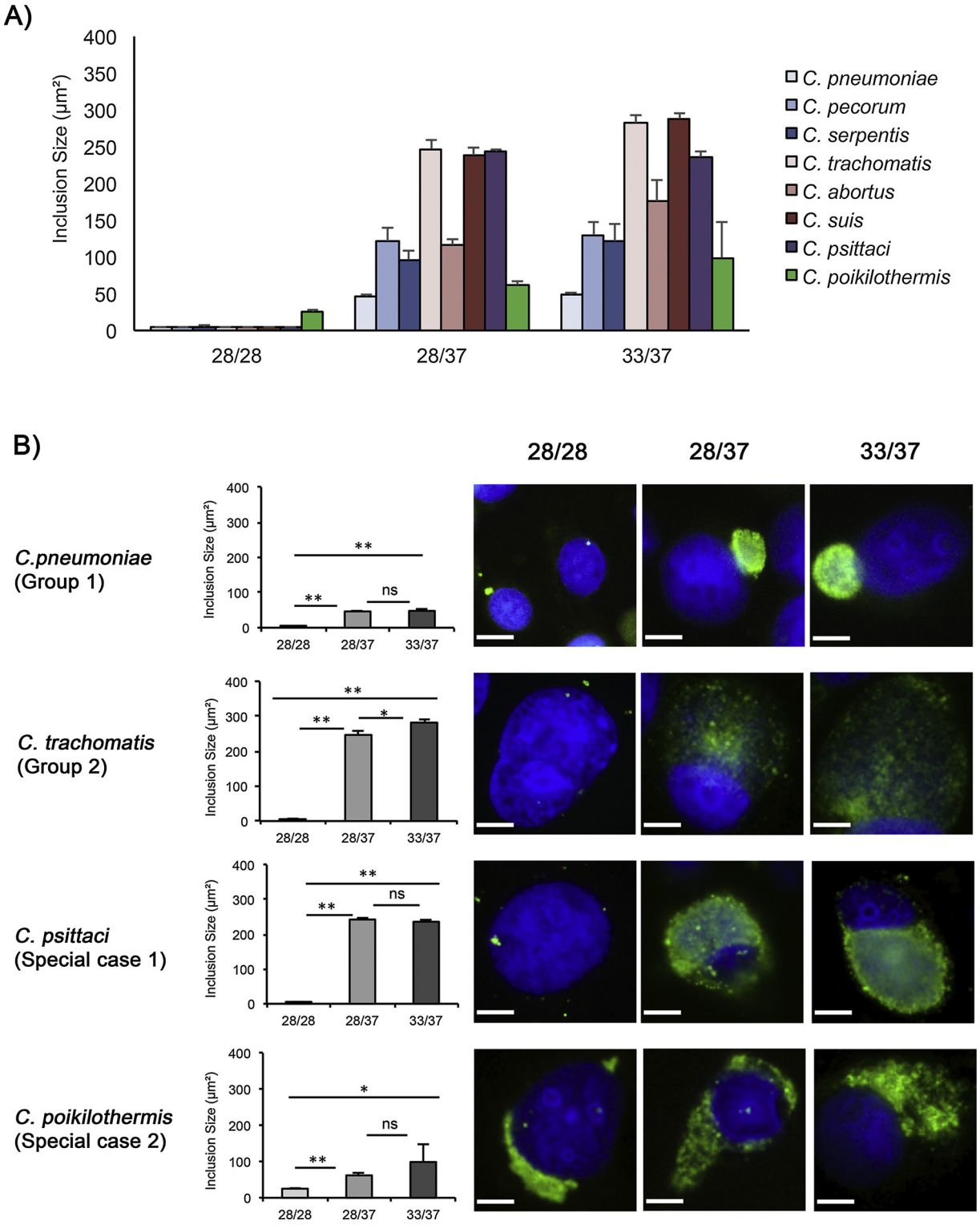

Fig. 1. The average inclusion size was significantly reduced at an incubation temperature of 28 °C compared to 37 °C A) From left to right, shown are Group 1 in blue (*C. pneumoniae* K6 [light blue], *C. pecorum* PV7855 [medium blue], *C. serpentis* H15-1957-10C [dark blue]), Group 2 in red (*C. trachomatis* serovar E [light red], *C. abortus* S26/3 [medium red], *C. suis* 5-27b [dark red]), special cases *C. psittaci* 6BC (purple) and *C. poikilothermis* S15-834 K (green). The inclusion size of fifty inclusions was measured per strain and condition (28/28, 28/37, 33/37) with a Leica DMLB fluorescence microscope (mean ± standard deviation, n = 3). **B)** Shown are the inclusion size measurements of *C. pneumoniae* representing Group 1, *C. trachomatis* representing Group 2, and special cases *C. psittaci* and *C. poikilothermis* at 48 hpi (left panel). Asterisks indicate statistical significance (ns = not significant; *p < 0.05; **p < 0.01) by Welch *t*-test (mean ± standard deviation, n = 3). Representative immunofluorescence images illustrate the morphology at 48 hpi (right panel). The size bar indicates 5 µm. Chlamydial inclusions are shown in green, the LLC- MK2 nuclei (DAPI) are shown in blue.

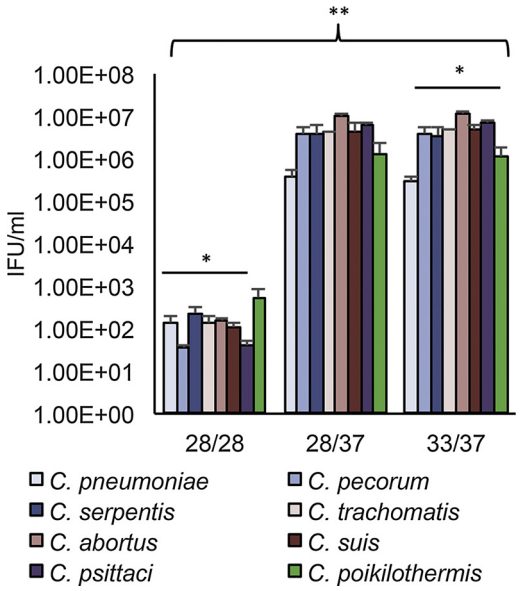

Fig. 2. Incubation at 28 °C significantly reduces chlamydial infectivity compared to 37 °C. The number of inclusions in 30 random microscopic fields was determined for duplicate coverslips per condition (28/28, 28/37, 33/37) using a Leica fluorescence microscope at 200x magnification with a 20x objective (PL FLUOTAR 20x/0.50 PH 2, '/0.17/B). Inclusion forming units (IFU/ml) are shown in a logarithmic scale. Asterisks indicate statistical significance (ns = not significant; *p < 0.05; **p < 0.01) by Welch *t*-test (mean ± standard deviation, n = 3).

3.2. Incubation at 28 °C significantly reduces chlamydial infectivity compared to 37 °C

Titration by sub-passage was performed to determine the infectivity of each strain per condition and was expressed as inclusion forming units per ml (IFU/ml). Titers confirmed previous observations regarding inclusion size and morphology by demonstrating that the infectivity of all strains was significantly higher at 37 °C of incubation ($3.77*10^5$ - $1.16*10^7$ IFU/ml) compared to 28/28 ($3.47*10^1$ – $5.41*10^2$ IFU/ml). Further confirming inclusion size data, *C. poikilothermis* appeared to be more infectious at 28/28 ($5.41*10^2 \pm 2.85*10^2$ IFU/ml) compared to all other strains at the same condition ($3.47*10^1$ - $2.34*10^2$), even though this finding was not significant (Fig. 2). These findings again contrast with our previous study (Staub et al., 2018), where the infectivity of *C. poikilothermis* was significantly reduced at 37 °C compared to incubation at 28 °C, while the titer data of *C. pneumoniae* and *C. serpentis* was confirmed in this present study.

Interestingly, the significantly different inclusion size between 28/37 and 33/37 detected for Group 2 (*C. trachomatis, C. suis, C. abortus*) was not reflected by titer analysis (Fig. 2, Fig. S3).

3.3. Ultrastructural analysis and morphology (TEM) of eight Chlamydia species 48 hpi

Generally, exposure to an incubation temperature of 28 °C appeared to slow down but not entirely arrest the developmental cycle of most chlamydial strains.

3.3.1. TEM analysis of C. pneumoniae, C. pecorum and C. serpentis (Group 1) revealed no EBs at an incubation temperature of 28 °C, and fully developed inclusions at 37 °C

The ultrastructural morphology of *C. pneumoniae* showed a small number of chlamydial bodies at 28/28 (n = 54), compared to 28/37 and 33/37, where the number of chlamydial bodies significantly increased (n = 1032 at 28/37, n = 842 at 33/37). Ultrastructural morphology further revealed small inclusions and no EBs at 28/28, only IBs (2%), dividing RBs (18%) and RBs (80%). In contrast, at 28/37 and 33/37, we observed fully developed inclusions with EBs (19% at 28/37, 16% at 33/37), IBs (21% at 28/37, 13% at 33/37), dividing RBs (12% at 28/37, 14% at 33/37) and RBs (48% at 28/37, 57% at 33/37). There was no sign of AB formation in any of the conditions at 48 h post infection (Fig. 3). Similar results were obtained in a previous study (Staub et al., 2018), where ultrastructural morphology of *C. pneumoniae* showed small, RB-dominant inclusions at 28 °C and fully developed inclusions containing EBs, RBs and IBs at 37 °C.

Similarly, there were small numbers of chlamydial bodies at 28/28 for *C. pecorum* (n = 73), compared to 28/37 and 33/37, where the number was significantly increased (n = 667 at 28/37, n = 2064 at 33/37). The ultrastructural morphology showed smaller inclusions at 28/28 with few EBs (2%), dividing RBs (12%) and RBs (85%), compared to 28/37 and 33/37 where we observed fully developed inclusions consisting of EBs (4% at 28/37, 31% at 33/37), IBs (20% at 28/37, 24% at 33/37), dividing RBs (10% at 28/37, 7% at 33/37) and RBs (64% at 28/37, 38% at 33/37). Moreover, we observed a small number of ABs at 28/28 (1%) and 28/37 (2%) compared to 33/37 (no ABs detected). The last strain in this group, *C. serpentis*, revealed a small number of chlamydial bodies at 28/28 (n = 82) compared to a significant increase at 28/37 (n = 1502) and 33/37 (n = 995). The ultrastructure of this strain was similar to that of *C. pneumoniae* with smaller inclusion at 28/28 containing few EBs (1%), dividing RBs (33%) and RBs (66%), compared to fully developed inclusions at 28/37 and 33/37 with more EBs (11% at 28/37, 10% at 33/37), IBs (17% at 28/37, 11% at 33/37), dividing RBs (12% at 28/37, 14% at 33/37) and RBs (60% at 28/37, 65% at 33/37). No AB formation was observed in any of the conditions (Fig. 3). Similarities between the ultrastructural morphology of *C. serpentis* and *C. pneumoniae* were already described in a very recent publication (Staub et al., 2018). In that study, RB-dominance following incubation at 28 °C and fully developed inclusions at 37 °C were described for both species. The close phylogenetic relationship between these two species may account for similar behavior *in vitro* (Staub et al., 2018).

Overall, of the three strains belonging to Group 1, only *C. pecorum* revealed a small number of ABs at 28/28 (1%) and 28/37 (2%), confirming a previous study of Kaltenboeck and Storz (1992), where three *C. pecorum* strains (1920BRZ, L1, R106), isolated from swine, showed AB formation at 42 h post infection. The phenomenon of spontaneous AB formation has been found, moreover, in the gastrointestinal tract of pigs that were experimentally infected with *C. suis* (Pospischil et al., 2009). In this present study, we found no indication for spontaneous AB formation in *C. suis* at any of the conditions investigated.

3.3.2. TEM analysis of C. trachomatis, C. abortus and C. suis revealed mild ultrastructural differences between the strains of Group 2

The analysis of Group 2 revealed that for *C. trachomatis*, the number of chlamydial bodies continuously increased from 28/28 to 33/37 (n = 1805 at 28/28, n = 1991 at 28/37, n = 3292 at 33/37), although the difference was not significant. Further analysis showed that *C. trachomatis* serovar E formed fully developed inclusions at all conditions with EBs (9% at 28/28, 47% at 28/37, 37% at 33/37), IBs (26% at 28/28, 17% at 28/37, 25% at 33/37), dividing RBs (7% at 28/28, 3% at 28/37, 4% at 33/37) and RBs (58% at 28/28, 33% at 28/37, 34% at 33/37), although the number of EBs was notably smaller at 28/28. For *C. abortus*, the number of chlamydial bodies significantly increased from 28/28 to 33/37 (n = 357 at 28/28, n = 1543 at 28/37 and n = 3059 at 33/37) with no EBs, 4% IBs, 18% dividing RBs and 78% RBs at 28/28. In contrast, the relative proportion of EBs was 35%, ˜20% IBs, 5–10% dividing RBs and ˜20% RBs for both 28/37 and 33/37. *C. suis*, the last representative of Group 2, presented only very few chlamydial bodies at 28/28 (3 RBs in 10 representative TEM images) compared to 28/37 (n = 1130) and 33/37 (n = 1017). Ultrastructural analysis further revealed that inclusions were fully developed at 28/37 and 33/37 with EBs (56% at 28/37, 47% at 33/37), IBs (12% at 28/37,

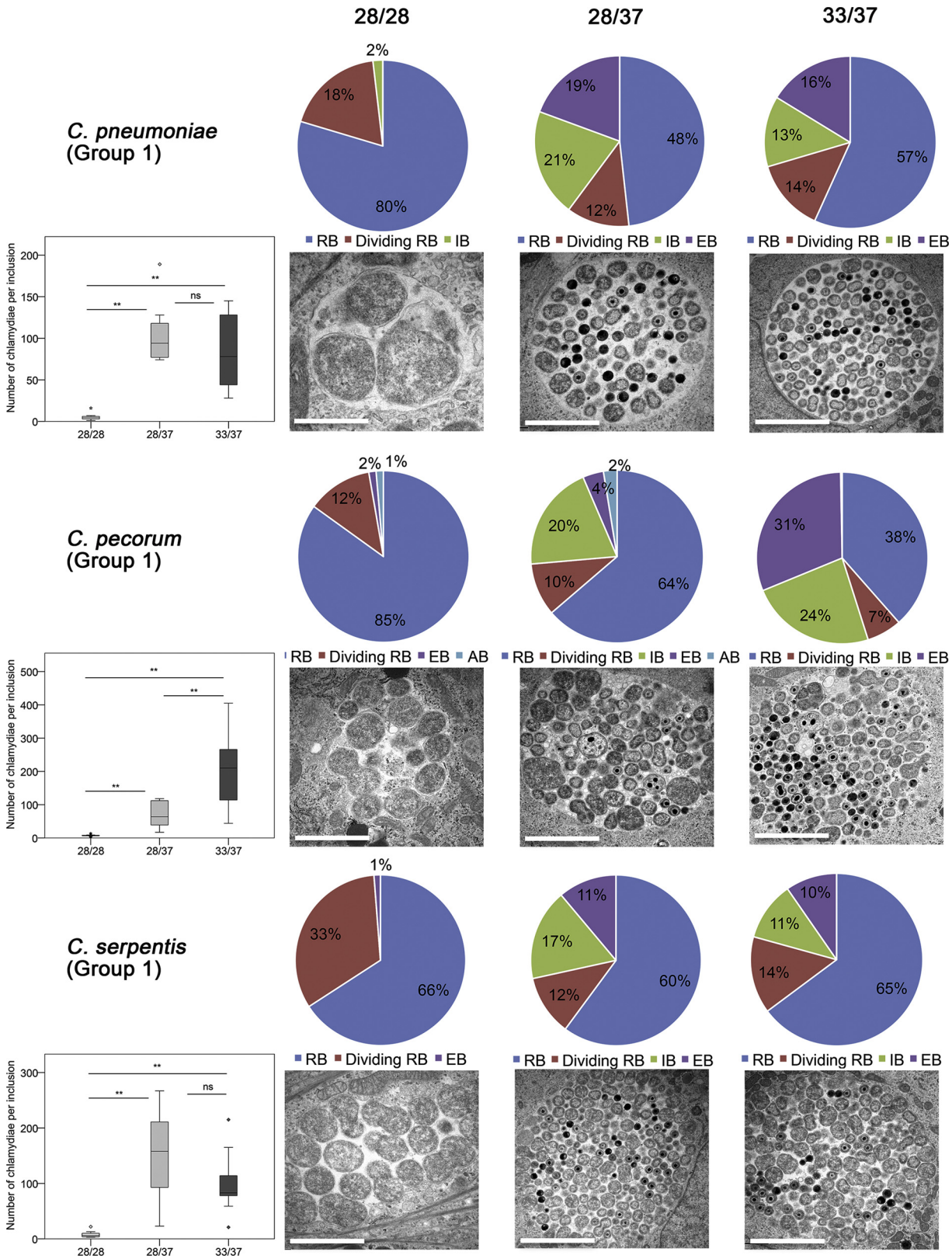

Fig. 3. TEM analysis of *C. pneumoniae* (top panel), *C. pecorum* (middle panel) and *C.serpentis* (bottom panel) (Group 1) revealed no EBs at an incubation temperature of 28 °C, and fully developed inclusions at 37 °C. Shown is a boxplot comparing the number of chlamydial particles per inclusion for each condition (left panel). Filled diamonds represent outliers (> 1.5x interquartile range), while grey asterisks represent extreme values (> 3x interquartile range). Boxplots were created by the SPSS Statistics software. Black asterisks indicate statistical significance (ns = not significant; *p < 0.05; **p < 0.01) by Welch *t*-test. The relative proportion of each developmental stage consisting of elementary bodies (EBs [dark grey]), intermediate bodies (IBs [medium grey]), dividing reticulate bodies (dividing RBs [medium to dark grey]), reticulate bodies (RBs [light grey]) and aberrant bodies (ABs [black]) is shown as a pie chart for each condition (top right panel). Representative images are shown in the bottom right panel. The size bar indicates 2 µm.

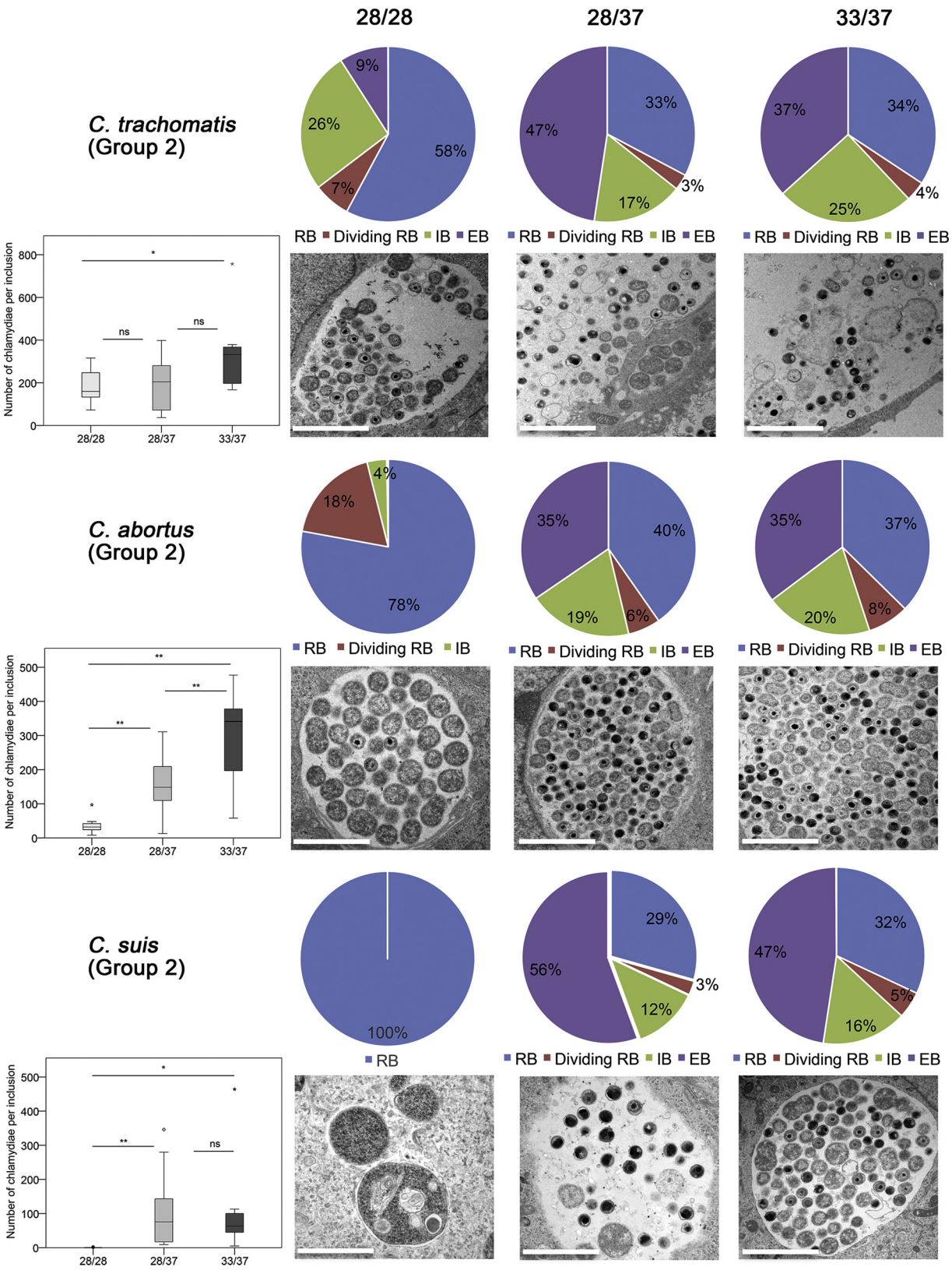

Fig. 4. TEM analysis of *C. trachomatis* (top panel), *C. abortus* (middle panel) and *C. suis* (bottom panel) revealed mild ultrastructural differences between strains of Group 2. Shown is a boxplot comparing the number of chlamydial particles per inclusion for each condition (left panel). Filled diamonds represent outliers (> 1.5x interquartile range), while grey asterisks represent extreme values (> 3x interquartile range). Boxplots were created by the SPSS Statistics software. Black asterisks indicate statistical significance (ns = not significant; *$p < 0.05$; **$p < 0.01$) by Welch *t*-test. The relative proportion of each developmental stage consisting of elementary bodies (EBs [dark grey]), intermediate bodies (IBs [medium grey]), dividing reticulate bodies (dividing RBs [medium to dark grey]), reticulate bodies (RBs [light grey]) and aberrant bodies (ABs [black]) is shown as a pie chart for each condition (top right panel). Representative images are shown in the bottom right panel. The size bar indicates 2 µm.

16% at 33/37), dividing RBs (3% at 28/37, 5% at 33/37) and RBs (29% at 28/37, 32% at 33/37). Furthermore, we observed no AB formation at 48 h post infection regardless of strain and condition for group 2 (Fig. 4). Given their close phylogenetic relationship (Seth-Smith et al., 2017), it was not surprising to find certain parallels in the behavior of *C. trachomatis* and *C. suis in vitro*. These common features are further stressed by the reported experimentally induced recombination between the two species following co-infection *in vitro* and the successful maintenance of *C. suis* genes in *C. trachomatis* recombinants for subsequent generations (Jeffrey et al., 2013; Suchland et al., 2009). In contrast to these similarities, *C. suis* appeared to be more sensitive to low temperatures than *C. trachomatis.* However, several strains of both species, *C. trachomatis* and *C. suis,* would have to be compared in order to confirm this observation. Such follow-up studies would need to include both tetracycline resistant and sensitive strains from the two previously described *C. suis* clades (Seth-Smith et al., 2017) as well as genital and ocular strains from the trachoma biovar and strains from the lymphogranuloma venereum (LGV) biovar. *C. abortus*, like all other strains tested in this study, belongs to the same genus as *C. suis* and *C. trachomatis*, but phylogenetically, they are quite diverse (Seth-Smit et al., 2017). While *C. psittaci* appears to be the evolutionary ancestor of *C. abortus* before it adapted to small ruminants (Van Loock et al., 2003), only few phenotypic parallels between the two strains were found in this study. Little is known about the effect of suboptimal temperatures on *C. abortus*, but its infectious EBs are able to remain viable in the environment for several days and, if the temperature is close to or below freezing, for months (Longbottom and Coulter, 2003). While we cannot confirm this experimentally, we observed that *C. abortus* remains infectious and forms viable inclusions at an incubation temperature of 28 °C for two days.

3.3.3. C. psittaci (special case 1) contains the highest proportion of EBs across all investigated strains

For *C. psittaci*, the number of chlamydial bodies significantly increased from 28/28 (n = 1934) to 33/37 (n = 2761 at 28/37, n = 2828 at 33/37). Ultrastructural morphology revealed fully developed inclusions at all conditions, though the number of EBs increased from 28/28 (32%) to 33/37 (71% at 28/37, 76% at 33/37), while the proportion of IBs (16% at 28/28, 8% at 28/37, 9% at 33/37), dividing RBs (6% at 28/28, 1% at 28/37, 1% at 33/37) and RBs (46% at 28/28, 20% at 28/37, 14% at 33/37) decreased. This was by far the highest proportion of EBs observed at 48 h across all investigated strains indicating that *C. psittaci* 6BCE has a faster developmental cycle compared to the other strains. AB formation was not observed (Fig. 5). Depending on the chlamydial species and strain, the developmental cycle usually takes between 48 to 72 h during an *in vitro* infection (AbdelRahman and Belland, 2005), but in this study, *C. psittaci* appeared to have a faster developmental cycle with EB predominance at 48 hpi. Apart from *C. psittaci*, such a rapid growth has only been reported for *C. trachomatis* serovar L2, which showed numerous inclusions already at 36 h post inoculation in contrast to *C. trachomatis* serovar E, which required approximately 72 to 96 h to complete its developmental cycle (Davis and Wyrick, 1997).

3.3.4. C. poikilothermis (special case 2) revealed fully formed, poorly demarcated inclusions at an incubation temperature of 28 °C

This strain showed no significant differences between the number of chlamydial bodies per condition (n = 1150 at 28/28, n = 1218 at 28/37, n = 873 at 33/37) and the ultrastructural analysis revealed fully developed inclusions for all conditions. Inclusions were poorly demarcated and appeared to grow around the nucleus in a crescent-like fashion as already described for immunofluorescence analysis. Akin to the other species, the proportion of EBs increased from 28/28 (3%) to 33/37 (17% at 28/37, 20% at 33/37), while the relative number of RBs decreased (76% at 28/28, 57% at 28/37, 58% at 33/37). The distribution of IBs (6% at 28/28, 19% at 28/37, 12% at 33/37) and dividing RBs (15% at 28/28, 7% at 28/37, 10% at 33/37) followed already described patterns in *C. pneumoniae*, *C. serpentis* and *C. abortus*. Similar to all previous strains, except *C. pecorum*, there was no sign of AB formation in any of the conditions investigated (Fig. 5). These findings stand in stark contrast to our previous study Staub et al. (2018), in which upon exposure to 37 °C, *C. poikilothermis* formed ABs as identified by immunofluorescence analysis and further confirmed by transmission electron microscopy. These findings were then further reflected by the already mentioned decreased infectivity at 37 °C compared to 28 °C. Surprisingly, we could not confirm these previous observations in this study, especially in view of the fact that *C. poikilothermis* stocks could only be grown at 28 °C in our laboratory (Staub et al., 2018). It could be possible that this chlamydial strain adapted to the higher temperature of 37 °C during additional passages that were performed between the previous and current study. Similar adaption processes comprising mutational changes during passaging have been reported in previous studies for *C. trachomatis* (Borges et al., 2013), however, these were long-term laboratory propagations and did not reveal changes in growth rates.

3.4. Conclusion

Upon analysis of inclusion size, titer and distribution of inclusion bodies (EBs, RBs, dividing RBs, IBs, ABs) per condition and strain, we found that all *Chlamydia* species are viable and grow at low incubation temperatures (28 °C), although optimal culture conditions appear to be at higher centrifugation (33 °C) and incubation (37 °C) temperatures. Many studies have been conducted *in vitro*, using different cell culture systems (Schiller et al., 2004), variable incubation temperatures (Kuo and Grayston, 1988; Donati et al., 2010; Joubert and Sturm, 2011; Staub et al., 2018; Mukhopadhyay et al., 2006; Wannaratana et al., 2017) and, in addition, various centrifugation temperatures (Borges et al., 2010; Staub et al., 2018; Wanninger et al., 2016; Marti et al., 2017), to improve the infection rate and increase the attachment of EBs to host cells (Prain and Pearce, 1989). In this study, we compared only the effect of centrifugation temperatures of 28 and 33 °C as well as incubation temperatures of 28 and 37 °C. As opposed to increased incubation temperatures (42 °C or 57 °C) (Mukhopadhyay et al., 2006; Wannaratana et al., 2017), no sign of the chlamydial stress response was found at 28 °C regardless of whether the preferred host was poikilothermic with a body temperature range of 6–32 °C (*C. serpentis*, *C. poikilothermis*; Amiel et al., 2011), a mammal with a range of 36.7–39.9 °C[1] (all other strains except *C. psittaci*; http://www.msdvetmanual.com) or birds (*C. psittaci*) with a range of 35.0–40.8 °C (Prinzinger et al., 1991). However, the broad host range of *C. psittaci* (birds, cattle, sheep, swine, horses, goats, cats and humans) and therefore a wide range regarding body temperature could explain its increased tolerance to temperatures below 30 °C. Moreover, it is not surprising that *C. poikilothermis* grows comparatively well at 28 °C, although there appear to be differences between recently isolated stock and stock that was stored at −80 °C for over 12 months. Further studies must be conducted to explain this observation.

Finally, we described two groups based on inclusion size data. While similarities between *C. pneumoniae, C. pecorum* and *C. serpentis* (Group 1) were not surprising based on their phylogenetic relationship, the observation that *C. abortus* grouped together with *C. suis* and *C. trachomatis* was unexpected. However, the group assignment was purely based on phenotypic observations gained in our study.

Future studies should further focus on the underlying mechanism of lower temperature influencing the chlamydial developmental cycle. Future studies would also need to include more strains from each species from different hosts, other chlamydial species such as *C. caviae*, *C.*

[1] https://www.msdvetmanual.com/special-subjects/reference-guides/normal-rectal-temperature-ranges

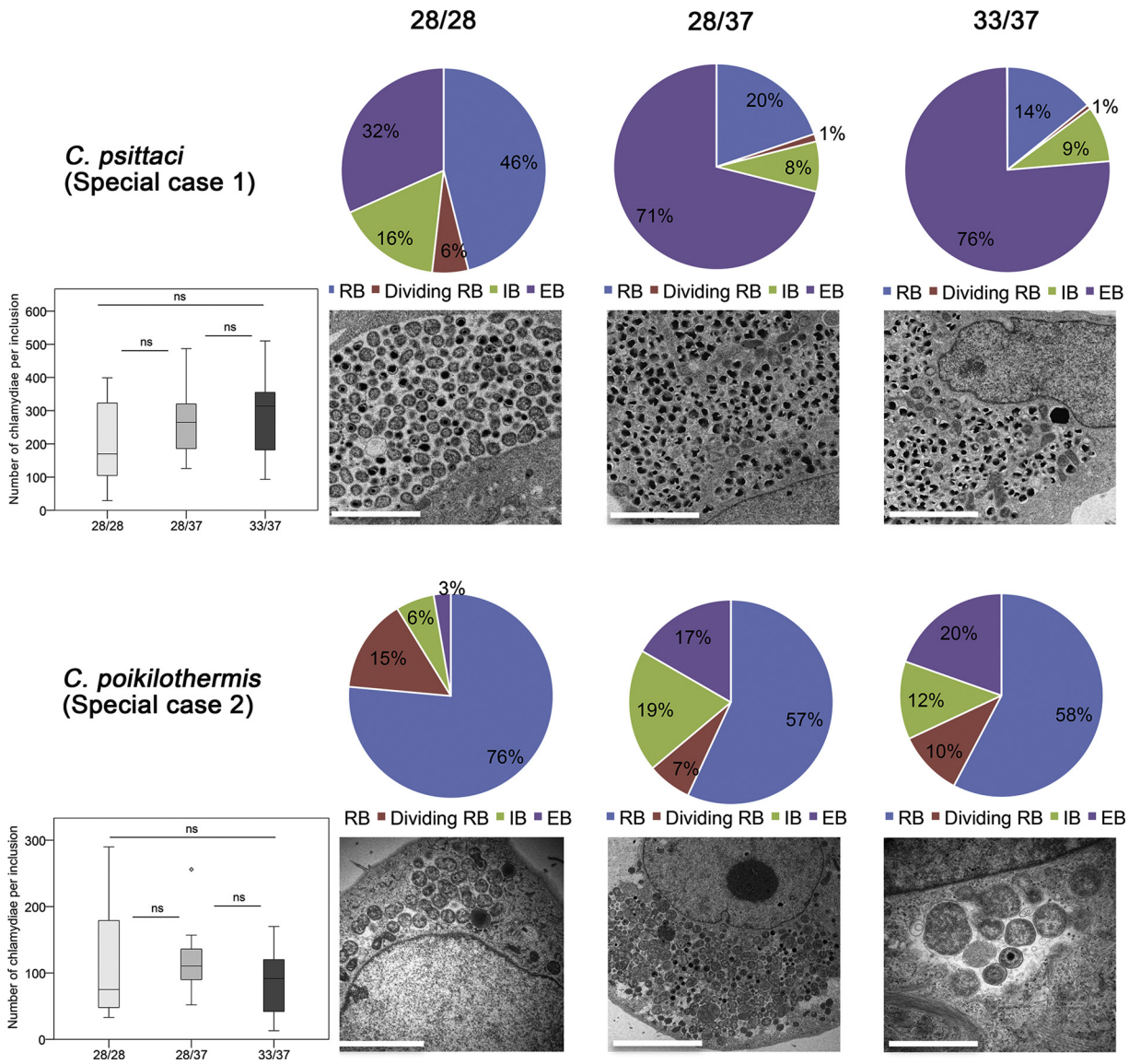

Fig. 5. *C. psittaci* (special case 1, top panel) contains the highest proportion of EBs across all investigated strains, while *C. poikilothermis* (special case 2, bottom panel) revealed fully formed, poorly demarcated inclusions at an incubation temperature of 28 °C. Shown is a boxplot comparing the number of chlamydial particles per inclusion for each condition (left panel). Filled diamonds represent outliers (> 1.5x interquartile range), while grey asterisks represent extreme values (> 3x interquartile range). Boxplots were created by the SPSS Statistics software. Black asterisks indicate statistical significance (ns = not significant; *p < 0.05; **p < 0.01) by Welch *t*-test. The relative proportion of each developmental stage consisting of elementary bodies (EBs [dark grey]), intermediate bodies (IBs [moderate grey]), dividing reticulate bodies (dividing RBs [moderate to dark grey]), reticulate bodies (RBs [light grey]) and aberrant bodies (ABs [black]) is shown as a pie chart for each condition (top right panel). Representative images are shown in the bottom right panel. The size bar indicates 2 µm.

felis, *C. muridarum*, *C. gallinacea* and *C. avium*, and experimental infections would need to be conducted in different cell lines as well as in the presence and absence of cycloheximide.

Conflict of interest statement

The authors declare that the research was conducted in the absence of any commercial or financial relationships that could be construed as a potential conflict of interest.

Author contributions statement

Substantial contribution to the conception and design of the work: DO, HM, MD, NB. Acquisition, analysis, interpretation of data: DO, HM, NB. Draft and/or critical revision of the manuscript: MD, HM, RB, AL, LN, BP, SR, NV, NB. Final approval of the version to be published: all authors agree to be accountable for all aspects of the work.

Acknowledgments

We would like to thank the laboratory team of the Institute of Veterinary Pathology, Zurich (IVPZ), for their technical assistance.

Appendix A. Supplementary data

Supplementary material related to this article can be found, in the online version, at doi:https://doi.org/10.1016/j.vetmic.2019.04.012.

References

AbdelRahman, Y.M., Belland, R.J., 2005. The chlamydial developmental cycle. FEMS Microbiol. Rev. 29, 949–959. https://doi.org/10.1016/j.femsre.2005.03.002.
Allan, I., Pearce, J.H., 1979. Modulation by centrifugation of cell susceptibility to

chlamydial infection. J. Gen. Microbiol. 111, 87–92. https://doi.org/10.1099/00221287-111-1-87.
Amiel, J.J., Chua, B., Wassersug, R., Jones, D.R., 2011. Temperature-dependent regulation of blood distribution in snakes. J. Exp. Biol. 214, 1458–1462. https://doi.org/10.1242/jeb.053934.
Borges, V., Ferreira, R., Nunes, A., Nogueira, P., Borrego, M.J., Gomes, J.P., 2010. Normalization strategies for real-time expression data in Chlamydia trachomatis. J. Microbiol. Meth. 82, 256–264. https://doi.org/10.1016/j.mimet.2010.06.013.
Borges, V., Ferreira, R., Nunes, Al., Sousa-Uva, M., Abreu, M., Borrego, M.J., Gomes, J.P., 2013. Effect of long-term laboratory propagation on Chlamydia trachomatis genome dynamics. Infect. Genet. Evol. 17, 23–32. https://doi.org/10.1016/j.meegid.2013.03.035.
Davis, C.H., Wyrick, P.B., 1997. Differences in the association of Chlamydia trachomatis serovar e and serovar L2 with epithelial cells in vitro may reflect biological differences in vivo. Infect. Immun. 65, 2914–2924.
Donati, M., Di Francesco, A., D'Antuono, A., Pignanelli, S., Shurdhi, A., Moroni, A., Baldelli, R., Cevenini, R., 2009a. Chlamydia trachomatis serovar distribution and other concurrent sexually transmitted infections in heterosexual men with urethritis in Italy. Eur. J. Clin. Microbiol. Infect. Dis. 28, 523–526. https://doi.org/10.1007/s10096-008-0650-z.
Donati, M., Laroucau, K., Storni, E., Mazzeo, C., Magnino, S., Di Francesco, A., Baldelli, R., Ceglie, L., Renzi, M., Cevenini, R., 2009b. Serological response to pgp3 protein in animal and human chlamydial infections. Vet. Microbiol. 135, 181–185. https://doi.org/10.1016/j.vetmic.2008.09.037.
Donati, M., Di Francesco, A., D'Antuono, A., Delucca, F., Shurdhi, A., Moroni, A., Baldelli, R., Cevenini, R., 2010. In vitro activities of several antimicrobial agents against recently isolated and genotyped Chlamydia trachomatis urogenital serovars d through K. Antimicrob. Agents Chemother. 54, 5379–5380. https://doi.org/10.1128/AAC.00553-10.
Escalante-Ochoa, C., Ducatelle, R., Haesebrouck, F., 2000. Dynamics of the development of Chlamydophila psittaci inclusions in epithelial and fibroblast host cells. J. Vet. Med. B Infect. Dis. Vet. Public Health 47, 343–349 doi: 0931-1793/2000/4705-0343$15.00/0.
Hatch, T.P., Miceli, M., Sublett, J.E., 1986. Synthesis of disulfide-bonded outer membrane proteins during the developmental cycle of Chlamydia psittaci and Chlamydia trachomatis. J. Bacteriol. 165, 379–385 doi: 0021-9193/86/020379-07$02.00/0.
Hodinka, R.L., Davis, C.H., Choong, J., Wyrick, P.B., 1988. Ultrastructural study of endocytosis of Chlamydia trachomatis by McCoy cells. Infect. Immun. 56, 1456–1463 doi:0019-9567/88/061456-08$02.00/0.
Jeffrey, B.M., Suchland, R.J., Eriksen, S.G., Sandoz, K.M., Rockey, D.D., 2013. Genomic and phenotypic characterization of in vitro-generated Chlamydia trachomatis recombinants. BMC Microbiol. 13, 142. https://doi.org/10.1186/1471-2180-13-142.
Joubert, B.C., Sturm, A.W., 2011. Differences in Chlamydia trachomatis growth rates in human keratinocytes among lymphogranuloma venereum reference strains and clinical isolates. J. Med. Microbiol. 60, 1565–1569. https://doi.org/10.1099/jmm.0.032169-0.
Kaltenboeck, B., Storz, J., 1992. Biological properties and genetic analysis of the ompA locus in chlamydiae isolated from swine. Am. J. Vet. Res. 53, 1482–1487.
Kuo, C.-C., Grayston, J.T., 1988. Factors affecting viability and growth in HeLa 299 cells of Chlamydia sp. Strain TWAR. J. Clin. Microbiol. 26, 812–815 doi:0095- 1137/88/050812-04$02.00/0.
Lee, C.K., 1981. Interaction between a trachoma strain of Chlamydia trachomatis and mouse fibroblasts (McCoy cells) in the absence of Centrifugation. Infect. Immun. 31, 584–591 doi:0019-9567/81/020584-08$02.00/0.
Lee, J.K., Enciso, G.A., Boassa, D., Chander, C.N., Lou, T.H., Pairawan, S.S., Guo, M.C., Wan, F.Y.M., Ellisman, M.H., Sütterlin, C., Tan, M., 2018. Replication-dependent size reduction precedes differentiation in Chlamydia trachomatis. Nat. Commun. 9, 45. https://doi.org/10.1038/s41467-017-02432-0.
Leonard, C.A., Schoborg, R.V., Borel, N., 2015. Damage/Danger associated molecular patterns (DAMPs) modulate Chlamydia pecorum and C. Trachomatis serovar e inclusion development in vitro. PLoS One 10https://doi.org/10.1371/journal.pone.0134943. e0134943.
Longbottom, D., Coulter, L.J., 2003. Animal chlamydioses and zoonotic implications. J. Comp. Pathol. Ther. 128, 217–244. https://doi.org/10.1053/jcpa.2002.0629.
Magnino, S., Vigo, P.G., Griffiths, P.C., Plater, J.M., Bazzocchi, C., De-Giuli, L., Bandi, C., Citterio, C.V., Garbarino, C., Fabbi, M., Genchi, C., 2000. Pneumonia infection in a chamois (*Rupicapra r. Rupicapra*) caused by *Chlamydophila pecorum* in an Italian regional park. Proceedings, 4th Meeting of the European Society for Chlamydia Research (Ed.: Pekka Saikku) 274.
Marti, H., Koschwanez, M., Pesch, T., Blenn, C., Borel, N., 2014. Water-filtered infrared a irradiation in combination with visible light inhibits acute chlamydial infection. PLoS One 9https://doi.org/10.1371/journal.pone.0102239. e102239.
Marti, H., Kim, H., Joseph, S.J., Dojiri, S., Read, T.D., Dean, D., 2017. Tet(C) gene transfer between Chlamydia suis strains occurs by homologous recombination after co-infection: implications for spread of tetracycline-resistance among Chlamydiaceae. Front. Microbiol. 8, 156. https://doi.org/10.3389/fmicb.2017.00156.
McClenaghan, M., Herring, A.J., Aitken, I., 1984. Comparison of Chlamydia psittaci isolates by DNA restriction endonuclease analysis. Infect. Immun. 45, 384–389 doi:0019-9567/84/080384-06$02.00/0.
Mukhopadhyay, S., Miller, R.D., Sullivan, E.D., Theodoropoulos, C., Mathews, S.A., Timms, P., Summersgill, J.T., 2006. Protein expression profiles of Chlamydia pneumoniae in models of persistence versus those of heat shock stress response. Infect. Immun. 74, 3853–3863. https://doi.org/10.1128/IAI.02104-05.
Pearce, J.H., 1986. Early events in chlamydial infection. Ann. Inst. Pasteur Microbiol. 137, 325–332. https://doi.org/10.1016/S0769-2609(86)80043-6.
Pospischil, A., Borel, N., Chowdhury, E.H., Guscetti, F., 2009. Aberrant chlamydial developmental forms in the gastrointestinal tract of pigs spontaneously and experimentally infected with Chlamydia suis. Vet. Microbiol. 135, 147–156. https://doi.org/10.1016/j.vetmic.2008.09.035.
Prain, C.J., Pearce, J.H., 1989. Ultrastructural studies on the intracellular fate of Chlamydia psittaci (Strain Guinea pig inclusion conjunctivitis) and Chlamydia trachomatis (Strain lymphogranuloma venereum 434): modulation of intracellular events and relationship with endocytic mechanism. J. Gen. Microbiol. 135, 2107–2123. https://doi.org/10.1099/00221287-135-7-2107.
Prinzinger, R., Prebmar, A., Schleucher, E., 1991. Body temperature in birds. Comp. Biochem. Physiol. 99, 499–506. https://doi.org/10.1016/0300-9629(91)90122-S.
Rockey, D.D., Fisher, E.R., Hackstadt, T., 1996. Temporal analysis of the developing Chlamydia psittaci inclusion by use of fluorescence and Electron microscopy. Infect. Immun. 64, 4269–4278.
Schiller, I., Schifferli, A., Gysling, P., Pospischil, A., 2004. Growth characteristics of porcine chlamydial strains in different cell sulture systems and comparison with ovine and avian chlamydial strains. Vet. J. 168, 74–80. https://doi.org/10.1016/S1090-0233(03)00039-X.
Seth-Smith, H.M.B., Wanninger, S., Bachmann, N., Marti, H., Qi, W., Donati, M., Di Francesco, A., Polkinghorne, A., Borel, N., 2017. The Chlamydia suis genome exhibits high levels of diversity, plasticity, and mobile antibiotic resistance: comparative genomics of a recent livestock cohort shows influence of treatment regimes. Genome Biol. Evol. 9, 750–760. https://doi.org/10.1093/gbe/evx043.
Spears, P., Storz, J., 1979. Biotyping of Chlamydia psittaci based on inclusion morphology and response to diethylaminoethyl-dextran and cycloheximide. Infect. Immun. 24, 224–232.
Staub, E., Marti, H., Biondi, R., Levi, A., Donati, M., Leonard, C.A., Ley, S.D., Pillonel, T., Greub, G., Seth-Smith, H.M.B., Borel, N., 2018. Novel Chlamydia species isolated from snakes are temperature-sensitive and exhibit decreased susceptibility to azithromycin. Sci. Rep. 8. https://doi.org/10.1038/s41598-018-23897-z.
Suchland, R.J., Sandoz, K.M., Jeffrey, B.M., Stamm, W.E., Rockey, D.D., 2009. Horizontal Transfer of Tetracycline Resistance among Chlamydia spp. In Vitro. Antimicrob. Agents Chemother. 53, 4604–4611. https://doi.org/10.1128/AAC.00477-09.
Van Loock, M., Vanrompay, D., Herrmann, B., Vander Stappen, J., Volckaert, G., Goddeeris, B.M., Everett, K.D.E., 2003. Missing links in the divergence of Chlamydophila abortus from Chlamydophila psittaci. Int. J. Syst. Evol. Microbiol. 53, 761–770. https://doi.org/10.1099/ijs.0.02329-0.
Wannaratana, S., Thontiravong, A., Amonsin, A., Pakpinyo, S., 2017. Persistence of Chlamydia psittaci in various temperatures and times. Avian Dis. 61, 40–45. https://doi.org/10.1637/11475-072216-Reg.
Wanninger, S., Donati, M., Di Francesco, A., Hässig, M., Hoffmann, K., Seth-Smith, H.M.B., Marti, H., Borel, N., 2016. Selective pressure promotes tetracycline resistance of Chlamydia suis in fattening pigs. PLoS One 11. https://doi.org/10.1371/journal.pone.0166917.